https://doi.org/10.46813/2025-157-163

MODELING THE CHARACTERISTICS OF ELECTRON AND SECONDARY PHOTONS BEAMS WHEN PASSING THROUGH AN AIR LAYER

E.V. Oleinikov[1], E.Yu. Remeta[1], O.I. Gomonai[1], Yu.Yu. Bilak[2]
[1]Institute of Electron Physics, NAS of Ukraine, Uzhhorod, Ukraine;
[2]Uzhhorod National University, Uzhhorod, Ukraine
E-mail: zheka.net.ua@gmail.com

Reliable information on the characteristics (spectral, integral, spatial distributions) of electron and secondary photons beams falling into the plane of sample potential placement during their irradiation using electron accelerators is necessary to ensure the optimization procedure (creation of homogeneous particle fields in the plane of sample placement) and prediction of experimental results (estimation of the absorbed dose during interaction with electrons and the contribution of additional dose from interaction with secondary photons). The results of simulations of the influence of air layers (1…5000 mm) between the electron output node of the M-30 microtron and the plane (1000 ×1000 mm) on the characteristics of the primary electron beam with an energy of 17.5 MeV and the generated secondary bremsstrahlung photons are presented. When modeling with the GEANT4 tool, the technical characteristics of the M-30 microtron were taken into account.

PACS: 29.17.+w, 29.27._a

INTRODUCTION

Beams of electron accelerators of various types are used to solve a wide range of applied problems related to various aspects of human life [1]. For the successful use of beams, reliable and accurate information about their initial characteristics (energy, spectral, integral, spatial distributions [2]), possible changes in these characteristics in the process of transporting particles to objects of irradiation and interacting with the irradiated materials themselves [3–6] is required. It should be noted that during the transportation of electrons in the air (between the accelerator output unit and the plane of potential placement of irradiated samples – hereinafter referred to as the plane), the processes of their collision, ionization, scattering, and bremsstrahlung occur [4, 6, 7]. Fig. 1 shows the energy dependence of the output of secondary photons formed during bremsstrahlung of monoenergetic electrons in air calculated by the NIST “ESTAR” program [4].

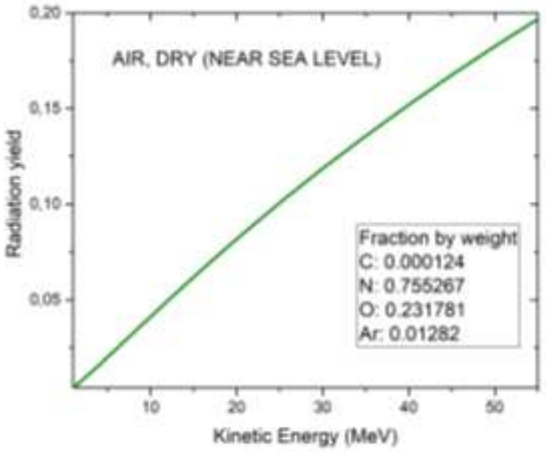

Fig. 1. Dependence of the bremsstrahlung photon yield on the electron energy [4]

The thickness of the air layer to the plane is determined depending on the geometric dimensions of the beams (increasing the distance to the samples is necessary to ensure the uniformity of the electron beam field [3]).

Reliable data on the content of secondary photons and their characteristics in electron beams of accelerators are extremely important for developing radiation technologies. These data are primarily necessary for developing innovative methods for minimizing the content of photons in electron beams [8] and forming mixed electron-photon fields during radiation treatment of irradiated objects [9–11]. These data are also necessary for developing experimental methods for determining the dosimetric characteristics of electron beams from the generated secondary radiation in cases where direct measurements of these quantities are impossible [2, 12, 13]. An example of such studies is using secondary photons generated by electron beams to determine their spectral and integral characteristics in the plane [14].

As a result of the analysis of the available experimental and theoretical studies of the influence of air on the change in the characteristics of electron beams and generated secondary photons, it was found that these changes are significantly determined by the parameters of the primary (initial) electron beam [2, 15]. Electron sources are defined by two main parameters: the output beam size and the average energy. They significantly affect the dosimetric characteristics of the beam during transportation in air to the plane [16]. The characteristics of the generated secondary photons also depend on the initial parameters of the electron beam [15]. Any differences between the characteristics of electron beams and generated secondary photons entering the plane for irradiation at different types of accelerators are caused by differences in the technical parameters of the output nodes, which affect the final shape of the resulting spatial distributions of particles [15, 17].

Therefore, for the successful use of electron accelerators to ensure the process of irradiation of samples and the possibility of predicting experimental results, reliable data for each type of accelerator on the characteristics of its beams (electrons and secondary photons) that interact with the objects of irradiation are required. These data are necessary for optimizing the irradiation process, namely: to obtain homogeneous fields of particles in the plane, taking into account their geometric dimensions, to reliably estimate (or determine) the absorbed dose during interaction with electrons, and the contribution of additional dose from interaction with secondary photons.

The purpose of the presented work was to study the influence of the air layer between the electron output node of the M-30 microtron and the plane in the potential placement of samples for irradiation on the change in the characteristics of the initial electron beams with an energy of 17.5 MeV and the generated secondary photons.

MATERIALS AND METHODS

To conduct Monte Carlo simulation of the characteristics of electron and secondary photons beams generated by them in the air layer (between the electron output node of the microtron and the plane of potential sample placement for irradiation, perpendicular to the electron beam axis), a program was developed in C++ using the GEANT4 v11.1 class library [18]. The program was implemented under the Windows platform with multi-threading [19].

The simulation was performed for the uncollimated electron beam with an initial energy of 17.5 MeV, since the use of additional structural elements in the sample irradiation schemes (for example, collimators, aligning filters) leads to further contamination of the electron beam with secondary (generated) particles – electrons and photons [20]. When performing the calculations, an equally probable distribution of the initial electron beam over the plane (ellipse shape with axes of 22 and 6 mm) was set [19, 21]. A photograph of the electron output unit into the air of the M-30 microtron of the Institute of Electron Physics of the NAS of Ukraine is presented in Fig. 2.

Fig. 2. Electron output unit of the M-30 microtron into the air

During the simulations, electrons and the bremsstrahlung photons generated by them, falling into the plane (1000x1000 mm) were recorded at 13 fixed distances (1, 50, 100, 500, 1000, 1500, 2000, 2500, 3000, 3500, 4000, 4500, and 5000 mm) between the electron output node into the air and the plane. When performing the calculations, the initial number of electrons was equal to 10^7. The results of the simulations, namely the energy spectra of electrons, secondary photons, and their integral values, were normalized to one initial electron.

RESEARCH RESULTS

As a result of the conducted computer experiment, the influence of the air layer between the electron output node of the M-30 microtron and the plane on the change in the spectral and integral characteristics of the initial electron beams and the secondary photons generated by them was investigated.

Thus, the energy spectra of electrons and generated secondary photons falling on the plane at different fixed distances of 1…5000 mm, i.e., and at different thicknesses of the air layers with which they interact, were established (Fig. 3).

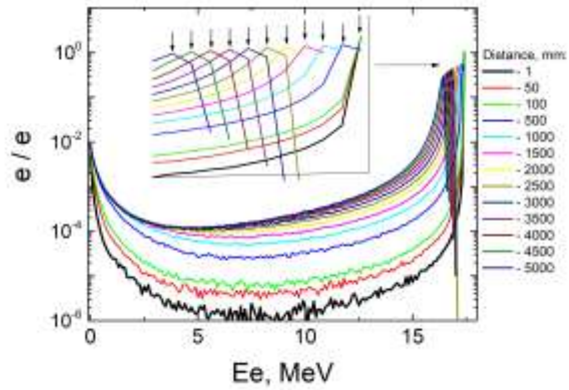

a

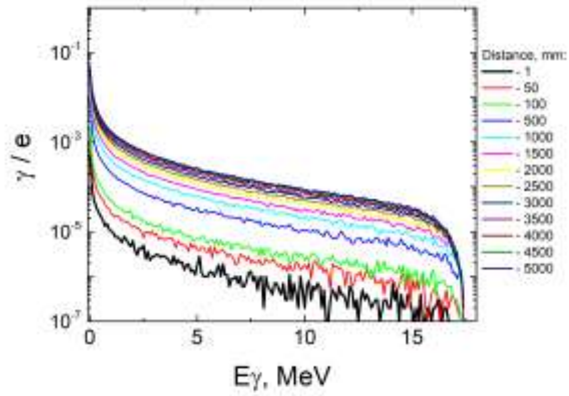

b

Fig. 3. Energy spectra of electrons (a) and secondary photons (b) incident on the plane (1000×1000 mm) at different distances

The obtained energy spectra of electrons and secondary photons were used to calculate their integral number (Fig. 4, Table):

$$N(E) = \int_0^{E_{max}} \phi(E) dE. \quad (1)$$

Here $\varphi(E)$ is the flux of particles (electrons, photons) with energy E.

The percentage of secondary photons in the electron beam was determined by the formula

$$C = \frac{N_\gamma}{N_e} \cdot 100\%, \quad (2)$$

where N_γ and N_e are the integral number of secondary photons and electrons calculated by formula (1), respectively.

Additionally, Table shows the percentage of secondary photons (2) in the electron beam at different distances.

Due to the interaction of the primary electron beam with air layers (collision, ionization, scattering, braking processes [4, 6, 22, 23]), significant changes in the characteristics of the primary (initial) electron beams and secondary photons generated in the air occur.

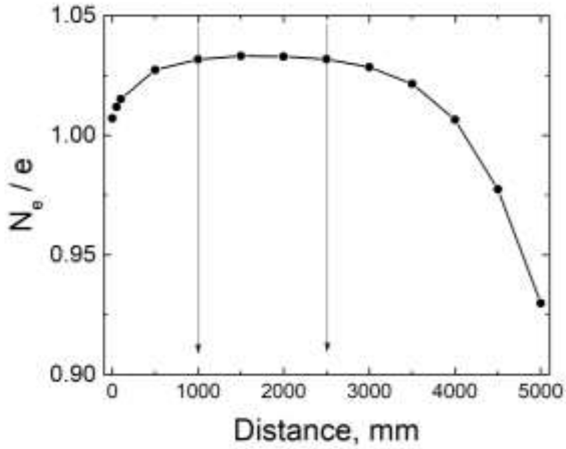

a

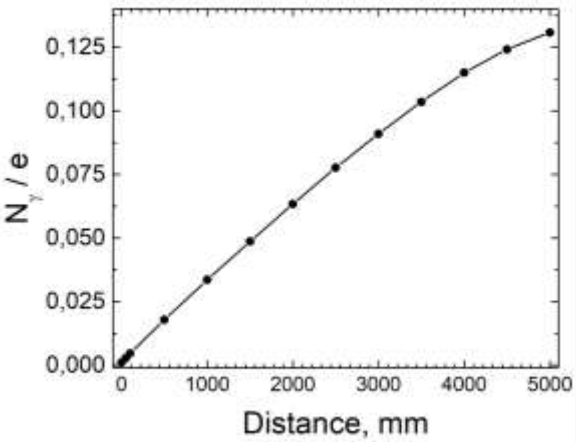

b

Fig. 4. Dependence of the integral number (1) of electrons (a) and secondary photons (b) falling into the 1000x1000 plane on the distance

As the distance to the plane increases from 1 to 5000 mm, the maximum energy of electrons entering the plane decreases from 17.5 to ~ 16.4 MeV (1 mm – 17.5 MeV, 1000 mm – ~17.2 MeV, 2000 mm – ~17.1 MeV, 3000 mm – ~16.8 MeV, 4000 mm – ~16.6 MeV, 5000 mm – ~16.4 MeV).

The integral number of electrons falling into the plane also significantly depends on the distance to it. Thus, these values increase from 1 to ~ 1000 mm; remain practically the same in the range 1000…2500 mm, and decrease above 2500 mm.

Increasing the distance to the plane enhances the probability of secondary photon generation due to the process of bremsstrahlung of electrons in the air. The integral number of the generated secondary photons increases by ~ 128 times with increasing distance from 1 to 5000 mm. Therefore, the thickness of the air layer affects them.

The content of secondary photons in the electron beam increases from ~ 0.1 to ~ 12%.

Integral number (1) of electrons and secondary photons incident on the plane at fixed distances and percentage of secondary photons (2)

Distance, mm	Electrons total / e	Photons total / e	Photon % in beam
1	1.0071	0.0010	0.1012
50	1.0118	0.0028	0.2730
100	1.0151	0.0046	0.4501
500	1.0272	0.0179	1.7089
1000	1.0317	0.0336	3.1513
1500	1.0331	0.0487	4.4972
2000	1.0329	0.0633	5.7779
2500	1.0317	0.0776	6.9977
3000	1.0284	0.0910	8.1275
3500	1.0215	0.1035	9.2010
4000	1.0065	0.1150	10.2505
4500	0.9775	0.1242	11.2713
5000	0.9298	0.1308	12.3319

Additionally, an analysis of the content of electrons and secondary photons, differentiated by 9 energy intervals (0…2, 2…4, 4…6, 6…8, 8…10, 10…12, 12…14, 14…16, and 16…17.5 MeV) in the spectra (see Fig. 3) at 13 fixed distances to the plane was carried out. Based on the calculated integral number of electrons and secondary photons (see (1)), their percentage content in the energy spectra for these distances was determined:

$$N_S = \frac{\int_{E_S \min}^{E_S \max} \phi(E)dE}{\int_{0}^{E \max} \phi(E)dE} \cdot 100\%. \quad (3)$$

Here N_s – relative number of particles in energy intervals s (1…9); $E_{s\ min}$ and $E_{s\ max}$ – minimum and maximum energy values for s energy intervals, $\varphi(E)$ – energy spectra of electrons and secondary photons falling into the plane.

The calculation results are presented in Fig. 5.

The percentage content (3) of electrons in the spectra differentiated by the energy intervals at different distances is as follows:

for E_e = 0…2 MeV – increase from 0.6853 to 2.8457% (for 1…2500 mm) and approximately constant value from 2.8457 to 2.8185% (for 2500…5000 mm);

increase at all distances (1…5000 mm) for E_e = 2…4 MeV from 0.0086 to 0.32%, for 4…6 MeV from 0.0035 to 0.25%, for 6…8 MeV from 0.0029 to 0.3129%, for 8…10 MeV from 0.0028 to 0.4599%, for 10…12 MeV from 0.0041 to 0.7841%, for 12…14 MeV from 0.0072 to 1.7546%, for 14…16 MeV from 0.0192 to 12.0074% (maximum); for E_e = 16…17.5 MeV – reduction from 99.26 to 81.28% (for 1… 5000 mm).

Percentage content (3) of secondary photons in spectra differentiated by energy intervals at different distances:
decrease (at 1…2500 mm) for E_e = 0…2 MeV from 85.59 to 81.06% and for 16…17.5 MeV from 0.16 to 0.10%; increase (at 1…2500 mm) for E_e = 2…4 MeV from 6.32 to 8.22%, for 4…6 MeV from 3.03 to 4.02%, for 6…8 MeV from 1.92 to 2.48%, for 8…10 MeV from 1.12 to 1.64%, for 10…12 MeV from 0.82 to 1.12%, for 12…14 MeV from 0.52 to 0.81%, for 14…16 MeV from 0.4700 to 0.5311%; reduction (at 2500×5000 mm) for 14…16 MeV from 0.5311 to 0.5086%.

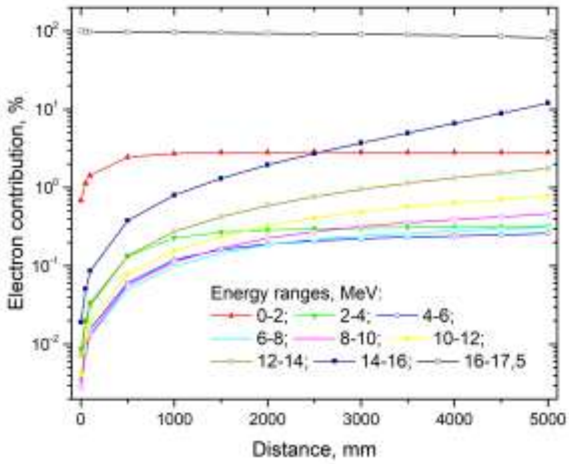

a

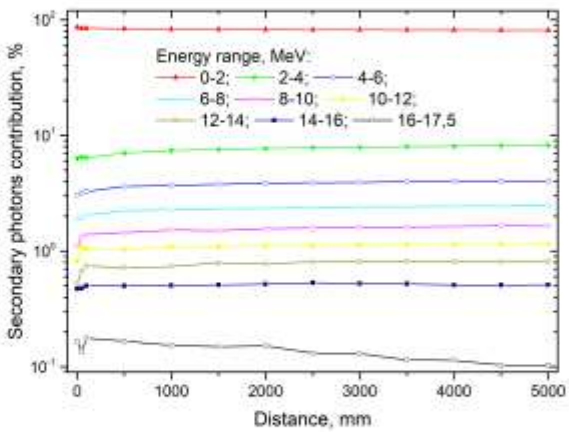

b

Fig. 5. Dependences of the percentage content (3) of electrons (a) and secondary photons (b), differentiated by energy intervals, on the distance

The simulation results allowed us to obtain profiles of electron beams and generated secondary photons in the section of the planes measuring 1000x1000 mm at fixed distances of 1000, 3000, and 5000 mm, presented in Fig. 6. It shows the probabilities of the distribution of electrons and secondary photons on the plane according to the inverse Gaussian cumulative distribution.

The obtained simulation results found that at a distance of 1000 mm from the output node, the highest concentration of electrons is located in the plane of an ellipse close to a circle with a radius of 40 mm. For secondary photons, this radius is 20 mm with a concentration twice as low as that of electrons. Further increase in the distance leads to a gradual increase in the uniformity of the distribution of the intensities of the electron and photon beams over the plane. This significantly reduces the number of particles that will hit the irradiated target if it is located on the beam axis.

The obtained results reflect the general patterns of the influence of air layers on the spectral, integral, and spatial distributions of primary electron beams and secondary photons. They are close to the available literature data [2, 15, 17, 24, 25] obtained on different types of accelerators. Any differences between the specified corresponding characteristics are caused by the technical parameters of the accelerators (electron output nodes into the air), which significantly affect the final parameters of electron beams and secondary photons in the plane of sample placement [2, 15, 17].

CONCLUSIONS

As a result of the simulations conducted by the created program using the GEANT4 toolkit, the influence of air layers (between the electron output node of the M-30 microtron and the potential plane of sample placement during their irradiation) on the change in the characteristics of the primary electron beam with an energy of 17.5 MeV and secondary photons was established for the first time.

The results obtained will allow using the electron accelerator of the IEF NAS of Ukraine – the M-30 microtron for:

- Optimizing the process of sample irradiation – obtain homogeneous particle fields in the plane of sample location, taking into account their geometric dimensions.

- Predicting the results of experimental studies – to make a reliable estimate of the absorbed dose during interaction with electrons and the contribution of additional dose from interaction with secondary photons.

This work was carried out within the framework of the topic “Excitation, ionization, luminescence of atomic and molecular systems under the action of photons and electrons”, State Registration No. – 0124U000782.

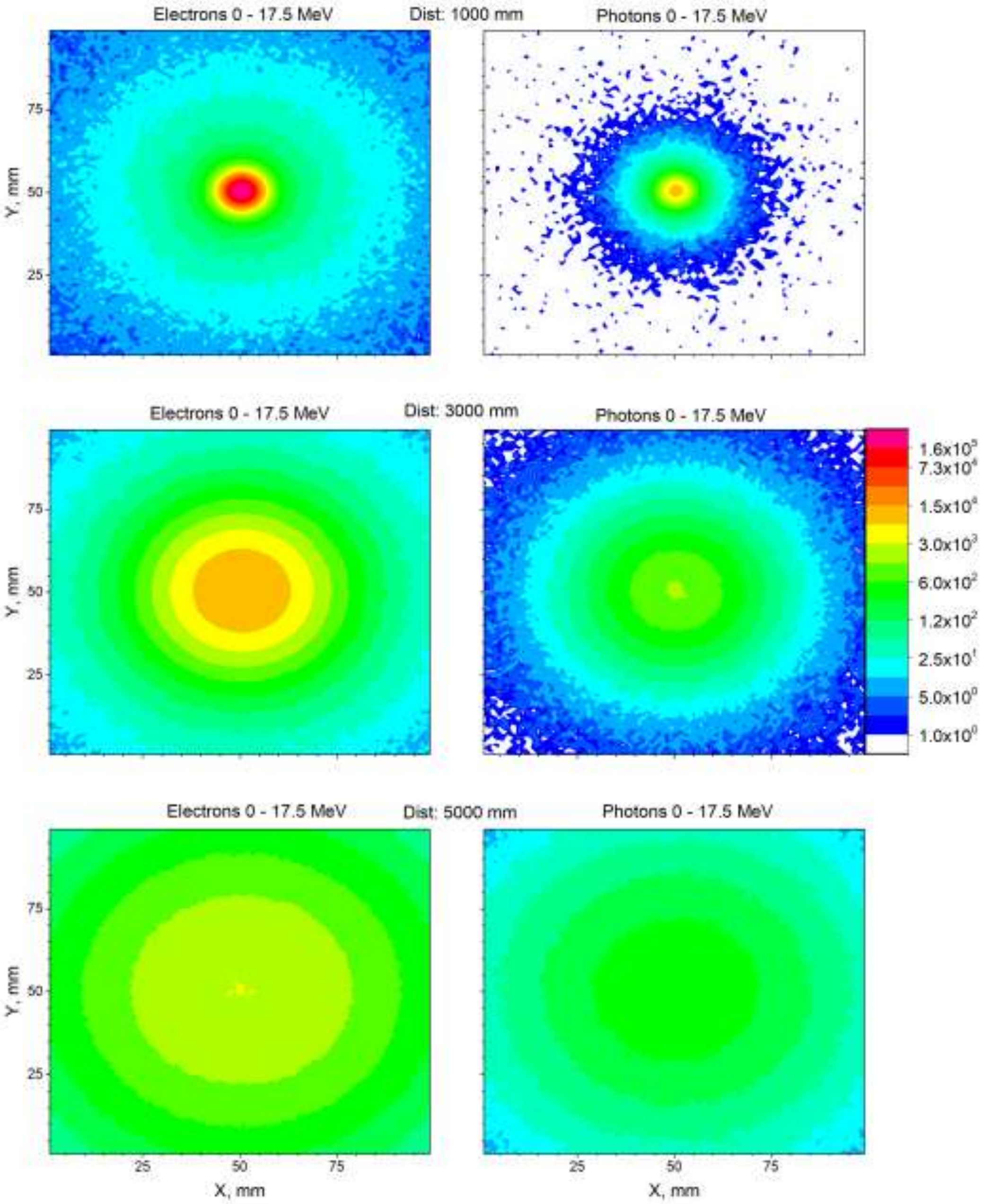

Fig. 6. Profiles of electrons (left) and secondary photons (right) incident on the plane at the fixed distances 1000, 3000, and 5000 mm

REFERENCES

1. A.G. Chmielewski. Radiation technologies: The future is today // *Radiation Physics and Chemistry.* 2023, v. 213, p. 111233.
2. A. Ryczkowski, T. Piotrowski, M. Staszczak, et al. Optimization of the regularization parameter in the dual annealing method used for the reconstruction of energy spectrum of electron beam generated by the AQURE mobile accelerator // *Zeitschrift für Medizinische Physik.* 2024, v. 34, issue 4, p. 510-520.
3. P. Apiwattanakul, S. Rimjae. Electron beam dynamic study and Monte Carlo simulation of accelerator-based irradiation system for natural rubber vulcanization // *Nuclear Inst. and Methods in Physics Research B*. 2020, v. 466, p. 69-75.
4. NIST ESTAR Database Program. https://physics.nist.gov/PhysRefData/Star/Text/ESTAR.html
5. Z. Yüksel, M.Ç. Tufan. Estimating the effect of electron beams interactions with the biological tissues //*Canadian Journal of Physics.* 2018, v. 96, No 12, p. 1338-1348.
6. M.K. Saadi, R. Machrafi. Development of a new code for stopping power and CSDA range calculation of incident charged particles, part A: electron and positron // *Applied Radiation and Isotopes*. 2020, v. 161, p. 109145.
7. H.O. Tekina, T. Manici, E.E. Altunsoy, et al. An artificial neural network-based estimation of bremsstrahlung photon flux calculated by MCNPX // *Acta Physica Polonica A.* 2017, v. 132, p. 967-969.

8. G.X. Ding, Z.(J) Chen, K. Homann. A scattering-foil free electron beam to increase dose rate for total skin electron therapy (TSET) // *Medical Physics.* 2024, v. 51, p. 5563-5571.
9. N. Khaledi, D. Sardari, M. Mohammadi, et al. Dosimetric evaluation of a novel electron–photon mixed beam, produced by a medical linear accelerator // *Journal of Radiotherapy in Practice*. 2018, v. 17, p. 319-331.
10. V.A. Shevchenko, A.Eh. Tenishev, V.L. Uvarov, A.A. Zakharchenko. Operation of an industrial electron accelerator in a double-beam e,X-mode // *Problems of Atomic Science and Technology.* 2019, v. 124, №6, p. 163-167.
11. V.L. Uvarov, A.A. Zakharchenko, L.V. Zarochintsev, et al. Analysis of a double-beam e,X-modeat an idustrial accelerator "EPOS" // *Problems of Atomic Science and Technology.* 2020, №3, p. 154-157.
12. R.I. Pomatsalyuk, V.A. Shevchenko, D.V. Titov, et al. Formation and monitoring of secondary x-ray radiation under product processing with electron beam // *Problems of Atomic Science and Technology.* 2021, №6(136), p. 201-205.
13. C. Oancea, K. Sykorova, J. Jakubek, et al. Dosimetric and temporal beam characterization of individual pulses in FLASH radiotherapy using Timepix3 pixelated detector placed out-of-field // *Physica Medica.* 2025, v. 129, p. 104872.
14. H. Kim, D.H. Jeong, S.K. Kang, et al. Real-time monitoring of ultra-high dose rate electron beams using bremsstrahlung photons // *Nuclear Engineering and Technology.* 2023, v. 55, p. 3417-3422.
15. A. Ryczkowski, B. Pawałowski, M. Kruszyna-Mochalska, et al. Commissioning, dosimetric characterisation and machine performance assessment of the AQURE mobile accelerator for intraoperative radiotherapy // *Polish Journal of Medical Physics and Engineering.* 2024, v. 30, p. 177-181.
16. L. Grevillot, T. Frisson, D. Maneval, et al. Simulation of a 6 MV Elekta precise linac photon beam using GATE/GEANT4 // *Phys. Med. Biol.* 2011, v. 56, p. 903-918.
17. H. Park, H.J. Choi, J.-I. Kim, C.H. Min. Analysis of dose distribution according to the initial electron beam of the linear accelerator: A Monte Carlo study // *Journal of Radiation Protection and Research*. 2018, v. 43, p. 10-19.
18. GEANT4 11.1 (9 December 2022). https://geant4.web.cern.ch/support/download
19. E.V. Oleinikov, I.V. Pylypchynets, O.O. Parlag, V.V. Pyskach. Photon and photoneutron outputs simulation from a tantalum converter at the M-30 microtron // *Problems of Atomic Science and Technology.* 2024, № 5(153), p. 148-153.
20. A. Toutaoui, A.N. Aichouche, K. Adjidir, A.C. Chami. In-air fluence profiles and water depth dose for uncollimated electron beams // *Journal of Medical Physics*. 2008, v. 33, p 141-146.
21. M. I. Romanyuk, J. J. Gaynish, O. M. Turhovsky, et al. Methods of formation and control of radiation fields of M-30 microtron // *Journal of Physical Studies.* 2022, v. 26, p. 1201.
22. S. Kahane. Backscattering of MeV Electrons. An Analysis of Tabata's experiment with Geant4 // *European Journal of Applied Physics*. 2022, v. 4, p. 48-56.
23. B. Koohi, R. Khabaz. Study of the backscattering of electron beams with energies typical of radiotherapy // *Physica Scripta.* 2022, v. 97, p. 125301.
24. G.X. Ding, Z.(J) Chen, K. Homann. A scattering-foil free electron beam to increase dose rate for total skin electron therapy (TSET) // *Medical Physics*. 2024, v. 51, p. 5563-5571.
25. G.X. Ding, S. Kucuker-Dogan, I.J. Das. Bremsstrahlung dose in the electron beam at extended distances in total skin electron therapy // *Medical Physics.* 2022, v. 49, issue 2, p. 1297-1302.

Article received 14.04.2025

МОДЕЛЮВАННЯ ХАРАКТЕРИСТИК ПУЧКІВ ЕЛЕКТРОНІВ І ВТОРИННИХ ФОТОНІВ ПРИ ПРОХОДЖЕННІ ШАРУ ПОВІТРЯ

Є.В. Олейніков, Є.Ю. Ремета, О.І. Гомонай, Ю.Ю. Білак

Достовірна інформація про характеристики (спектральні, інтегральні, просторові розподіли) пучків електронів та вторинних фотонів, що попадають у потенційну площину розміщення зразків при їх опромінені на прискорювачах, необхідна для забезпечення процедури оптимізації (створення однорідних полів частинок у площині розташування зразків) та прогнозування результатів експериментів (оцінки поглинутої дози при взаємодії з електронами та внеску додаткової дози від взаємодії з вторинними фотонами). Представлено результати моделювань впливу шарів повітря (1…5000 мм) між вузлом виводу електронів мікротрона М-30 та потенційною площиною (1000×1000 мм) на характеристики первинного пучка електронів з енергією 17,5 МеВ та згенерованих вторинних гальмівних фотонів. При моделюванні інструментарієм GEANT4 враховувалися технічні характеристики мікротрона М-30.